C h a p t e r 4

Efficient Syntheses of Linear and Cyclic Brush Polymers via Ring-Opening Metathesis Polymerization of Macromonomers

Portions of this chapter have been published: Xia, Y.; Kornfield, J. A.; Grubbs, R. H. *Macromolecules* **2009**, 42, 3761-3766.

Abstract

Various macromonomers (MMs) were efficiently synthesized through the copper-catalyzed "click" coupling of a norbornene moiety to the chain end of poly(methylacrylate), poly(*t*-butylacrylate), and polystyrene that were prepared using atom transfer radical polymerization. Ring-opening metathesis polymerization (ROMP) of these MMs was carried out using the highly active, fast-initiating ruthenium catalyst $(H_2IMes)(pyr)_2(Cl)_2RuCHPh$ in THF at room temperature. ROMP of MMs was found to be living with almost quantitative conversions (>90%) of MMs, producing brush polymers with very low polydispersity indices of 1.01−1.07 and high M_ns of 200−2600 kDa. The efficient ROMP of such MMs provides facile access to a variety of brush polymers and overcomes previous difficulties in the controlled polymerization of MMs. Atomic force microscopy (AFM) of the brush polymer products revealed extended, wormlike shapes as a result of significant steric repulsion of densely grafted side chains.

When cyclic catalysts were used to polymerize these MMs, cyclic brush polymers were clearly observed using AFM together with linear brush polymer impurities.

Introduction

With our knowledge of REMP mechanism on relatively simple monomers, we moved our attention to the confirmation of the cyclic topology of REMP polymers. Besides the chemical structure-based and property-based characterizations, the most convincing evidence would be to directly image cyclic polymers. However, flexible polymers adopt a random-coil conformation, making it impossible to distinguish different topologies when imaged. Therefore, the polymer backbone has to be forced to adopt an extended conformation and needs to be grafted with side chains to make it thicker and larger to facilitate molecular imaging. Bottle-brush polymer is ideal for this purpose. Brush polymers are a unique type of macromolecules with a high density of side chains grafted to the backbone.[1-3] The compact structure leads to an extended backbone conformation, causing the polymer to adopt a cylindrical or wormlike structure.[4,5] Furthermore, cyclic brush polymers provide a versatile molecular platform to build up cyclic organic nanostructures, which are otherwise difficult to obtain.

However, facile and precise control over the architecture, size, and functionality of brush polymers remains a central challenge. Brush polymers are usually prepared by three grafting methods: “grafting from”, “grafting onto”, and “grafting through” (ca. the macromonomer (MM) approach).[2,3] The “grafting from” approach involves the growth of side chains from backbone polymers with pendent initiation sites (macroinitiators). This approach and has been the most widely explored route to brush polymers, and a variety of monomers has been used for both the backbone and the side chain.[6-11] Importantly, the initiation efficiency from the macroinitiators may be limited due to the high density of initiation sites.[12,13] The “grafting onto” method has the advantage that it allows for

individual preparation of backbone polymers and side chains.[14-17] The downside is that grafting becomes progressively more difficult as conversion increases, leading to limited grafting density, even when a large molar excess of side chains is used.[16] Additionally, due to the ultrahigh MW of cyclic functionalized polynorbornenes (often >1 MDa) we prepared using REMP, "grafting from" and "grafting onto" these polynorbornenes all resulted in gigantic polymers that cannot be dissolved for any measurements.

Therefore, we focused on the MM approach. Among the three methods for preparation of brush polymers, only the MM approach guarantees complete grafting (i.e., one side chain per repeating unit). Additionally, the MM approach can afford the most precise and easiest control of side chain length and main chain length, provided that the polymerization of MM is efficient and controlled. However, synthesis of polymacromonomers (polyMM) with a high degree of polymerization (DP) and low polydispersity index (PDI) remains synthetically challenging, largely because of the inherently low concentration of polymerizable groups and the demanding steric hindrance of side chains.

Conventional radical polymerization of highly concentrated MM solution[18-20] and metallocene-catalyzed polymerization of MM[21,22] have been shown to yield high molecular weight (MW) polyMM, but with limited conversion and high PDI. Controlled radical,[23] anionic,[24] and metathesis polymerizations[25-30] of MMs have shown limited success, and only low DPs for the backbone of graft polymers were obtained. In several examples, ring-opening metathesis polymerization (ROMP) of MMs using early transition metals, such as molybdenum, has been used to produce narrowly dispersed polyMMs. However, the DP of the backbone of these polyMMs remained low (typically

5-20).[25-30] Therefore, these graft polymers were believed to resemble star architectures instead of brushlike structures. In addition, the limited functional group tolerance and air and moisture sensitivity of these catalysts narrow their applications. More recently, Ru-based catalyst **1** was used in the ROMP of MMs. Although narrowly dispersed graft polymers were obtained, the relatively low reactivity of **1** limited the DP of these graft polymers.[31,32] To our knowledge, there exists only one example of a *narrowly dispersed* polyMM with high MW, which was prepared by the ROMP of a polylactide norbornenyl MM using catalyst **1**.[33] Ru catalyst **2** shows greatly increased reactivity compared to **1**, but the resulting polymers are generally polydisperse due to its slow initiation.[34] We have recently reported on a class of pyridine-containing catalysts, including catalyst **3**, that mediate living polymerization. These catalysts exhibit both fast initiation and high reactivity.[35-37] Catalyst **3** has been shown to polymerize sterically demanding monomers, as Fréchet and co-workers have recently demonstrated the block copolymerization of dendronized norbornenes.[38] The fast initiation, high reactivity, and high functional group tolerance of catalyst **3** make it ideal for the polymerization of MMs.

The synthesis of MMs presents another challenge. Most of the reported preparations of norbornenyl MMs involve anionic polymerization using either a functionalized norbornene as the initiator[25,26] or end capping of a "living" polymer chain to install the norbornenyl group.[27-30] However, these routes generally require stringent experimental conditions and limit functionality in the polymer. Over the last fifteen years, controlled radical polymerization (CRP) has emerged as a powerful and versatile technique for the preparation of a variety of functionalized polymers with controlled MW and end group functionality.[39-41] Wooley and co-workers[42] and Advincula and co-

workers[43] have recently studied the syntheses of norbornenyl MMs by atom transfer radical polymerization (ATRP) and reversible addition–fragmentation chain transfer (RAFT) polymerization, respectively, using functionalized norbornenes as the initiator or chain transfer agent. However, the norbornenyl functionality led to bimodal MW distributions with high MW components in both the ATRP and the RAFT polymerization of acrylates even in large excess of monomer. This was attributed to the copolymerization of the norbornene functionality with acrylate monomers. Therefore, we sought a more versatile approach to obtain well-defined norbornenyl MMs prepared via CRP.

The combination of ATRP and "click" functionalization has been demonstrated to be a highly efficient way to synthesize polymers with controlled MW and desired end group functionality for subsequent modifications.[44-48] Recently, Sumerlin and co-workers reported the synthesis of MMs through the "click" coupling of azido-terminated polymers with propargyl (meth)acrylate with a high degree of end group functionalization.[49] Considering the reported compatibility of ruthenium catalysts with the triazole group resulted from the "click" reaction,[50] we sought to extend this approach to the preparation of a variety of norbornenyl MMs by coupling azido-terminated polymers made by ATRP with alkyne-functionalized norbornene. Herein, we report the facile synthesis of various high MW brush polymers with controlled MW and narrow PDI in both the side chain and the backbone from norbornenyl MMs that were prepared efficiently by ATRP and "click" functionalization.

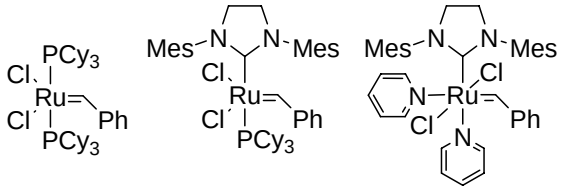

1 **2** **3**

Scheme 1. Ru-based metathesis catalysts.

Results and Discussion

Synthesis of Norbornenyl Macromonomers. Norbornene-based monomers (vs. cyclobutene or cyclooctene-based monomers) were chosen as the reactive group on the MMs due to their high ring strains, commercial availability, and the lack of chain transfer in ROMP. Particularly, *exo*-norbornenes were used in this study because they are known to exhibit significantly higher reactivity than their *endo*-norbornenyl analogs due to reduced steric hindrance at the olefin.[51-53]

To avoid the undesirable copolymerization of norbornene during the preparation of the side chains by ATRP, the norbornenyl functionality was attached to a pre-formed polymer chain end using copper catalyzed azide-alkyne "click" chemistry. *exo*-Norbornene monomer **4** bearing a terminal acetylene group was synthesized by condensation of *exo*-norbornene anhydride with 10-amino-1-decanol, followed by esterification with propargylacetic acid mediated by EDC/DMAP (Scheme 2). Both reactions gave clean products in good yields. The long alkyl spacer between norbornene and acetylene is designed to reduce the steric congestion during the ROMP of MMs.

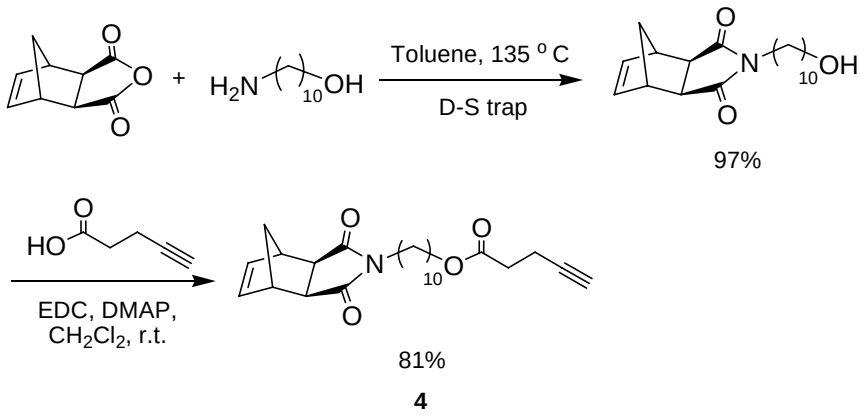

4

Scheme 2. Synthesis of monomer **4**.

ATRP of methyl acrylate (MA), *tert*-butyl acrylate (*t*BA) and styrene (St) were conducted using a CuBr/PMDETA catalytic system to produce a variety of side chain polymers with different MWs and functionalities. Polymerizations were stopped before 70% conversion was reached to retain the bromine chain-end functionality. Narrowly dispersed polymers were obtained in all cases, and their bromine end groups were subsequently transformed to azides quantitatively through nucleophilic substitution reaction with NaN_3 in DMF (Figure 1). Absolute polymer MWs were measured using GPC coupled with a multiangle laser light scattering (MALLS) detector (Table 1).

Next, the azido-terminated polymers were coupled with a stoichiometric amount of norbornene monomer **4** in THF at 50 ºC in the presence of a catalytic amount of CuBr with PMDETA as the ligand (Scheme 3). Regardless of the type of polymer or the MW, all ATRP polymers were furnished with norbornene end group quantitatively without the need for excess **4**. ^{1}H NMR spectroscopy clearly showed the end group transformation. When the terminal azide group was transformed to a triazole ring, the ω-terminal methine proton (H_a) resonance of the pre-polymer completely shifted from 3.9-4.0 ppm to 4.9-5.1 ppm for PS and from 3.7-3.8 ppm to 5.1-5.3 ppm for PMA and P*t*BA, respectively.

Concomitant appearance of signals from the norbornenyl moiety also confirmed that the desired reaction had taken place (Figure 1). The newly formed triazole proton was also observed to resonate at 7.4-7.5 ppm for PMA and P*t*BA, but was overlapped with broad aromatic proton signals in the case of PS. Integrations of norbornenyl olefin peak (H_e at 6.25 ppm) and the ω-terminal methine proton (H_a) peak gave a 2:1 ratio, indicating complete "click" coupling. Furthermore, the integrations of norbornenyl olefin and polymer backbone signals were compared to calculate the DP of the polymer. The DPs calculated by ^{1}H NMR spectroscopy (DP_{NMR}) were in good agreement with the DPs calculated by MALLS-GPC (DP_{GPC}), indicating an overall high degree of end group functionalization of these polymers (Table 1). Furthermore, the GPC peak shape of the pre-polymer and its corresponding MM remained unchanged. Interestingly, a difference in elution time of the GPC trace before and after "click" coupling could also be observed for smaller MMs (i.e., NB-PS, M_n = 2.2 kDa). The difference in their elution times may reflect the effect of the relatively large substituted norbornenyl end group (MW = 399.2 Da) on the size of the polymer coil.

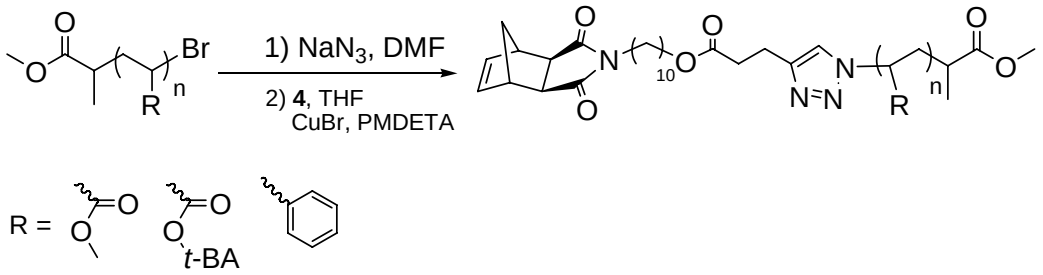

Scheme 3. Synthesis of macromonomers.

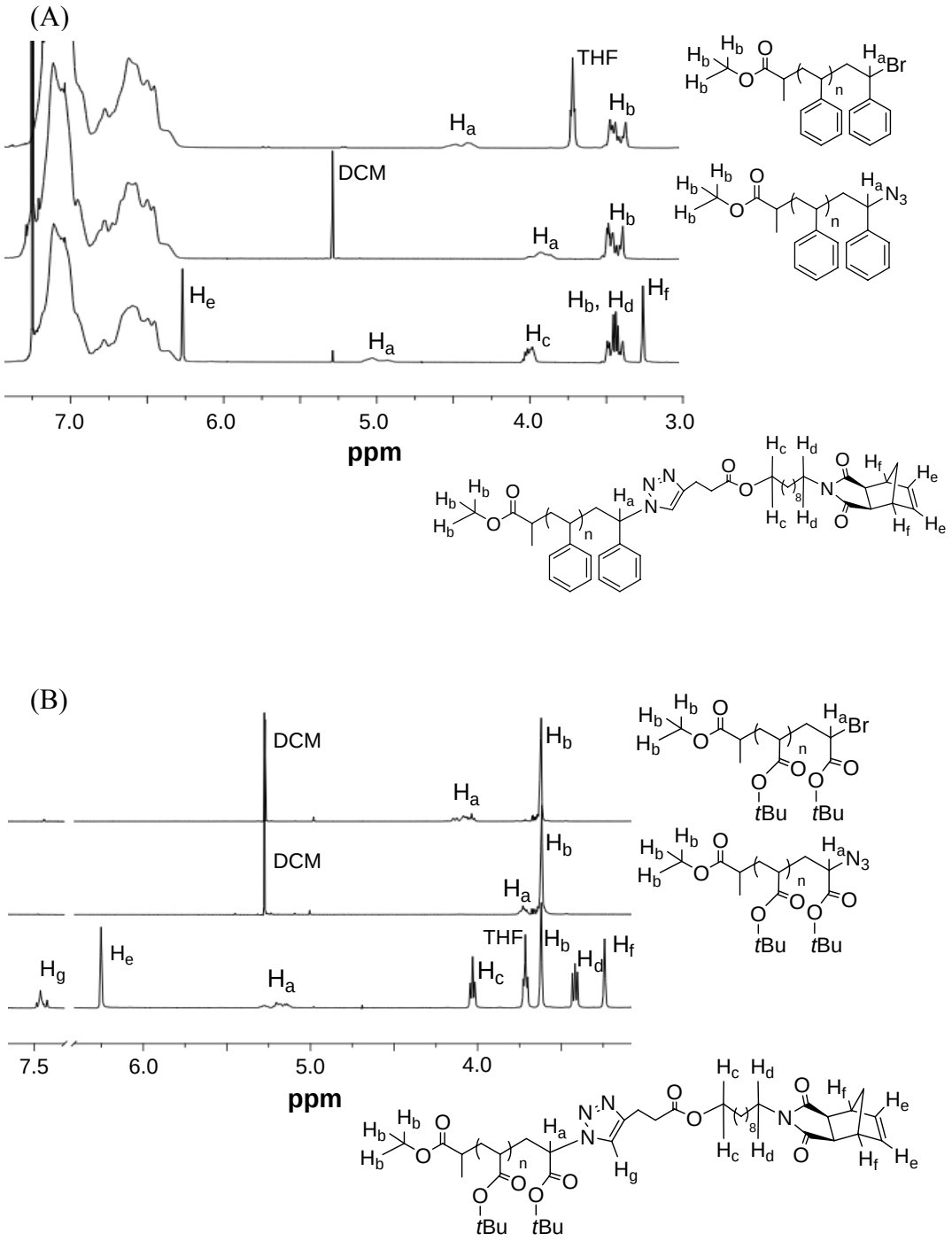

Figure 1. ^{1}H NMR spectra of end group transformations: (A) PS-Br (top), PS-N_3 (middle), NB(PS)2.2k (bottom); (B) P*t*BA-Br (top), PS-N_3 (middle), NB(P*t*BA)4.7k (bottom).

Table 1. Characteristics of ω-norbornenyl macromonomers

Sample name[a]	Polymer type	$M_{n,GPC}$[b] (kDa)	DP_{GPC}[c]	DP_{NMR}[d]	PDI[b]
NB(PMA)3.7k	PMA	3.7	38	36	1.03
NB(P*t*BA)4.7k	P*t*BA	4.7	33	33	1.03
NB(PS)2.2k	PS	2.2	17	19	1.03
NB(PS)6.6k	PS	6.6	60	66	1.02

[a]Macromonomers were named using a format of NB(X)Y, with X designating the type of pre-polymer and Y designating the M_n of macromonomer. [b]Determined by GPC in THF using RI and MALLS detectors. [c]Calculated by ($M_{n,GPC}$ − molar mass of **4** (399.2 Da)) / molar mass of monomer. [d]Calculated by comparing the integrations of norbornenyl olefin and polymer backbone proton signals from ^{1}H NMR spectra in $CDCl_3$.

ROMP of Macromonomers. We first investigated the ROMP of P*t*BA-macromonomer (P*t*BA-MM) as the *tert*-butyl group can be readily hydrolyzed to yield water soluble poly(acrylic acid) side chains, which can be used as polyelectrolytes and biomaterials, or further modified.[10] NB(P*t*BA)4.7k was dissolved in THF at 0.05 M, and catalyst **3** was injected from a stock solution at different MM to catalyst ratios ([M/C]) at room temperature. The solution became more viscous within a few minutes, and aliquots were withdrawn from the polymerization solutions at different time intervals and terminated immediately with excess vinyl ether. GPC analyses of the aliquots all showed narrow and monomodal peaks for the polyMM, and the MW increased linearly with conversion. The PDIs remained very low throughout the polymerization. Clean first-order kinetics were also observed from the linear logarithmic plots of conversion vs time ($\ln[M]_0/[M]_t$ vs time), indicating a constant concentration of propagating species (Figure 2). The polymerization rates measured by the slopes in the kinetic plot were also proportional to the catalyst loading (Figure 2C). The first-order kinetics and linear MW growth profile

both suggest that the living nature of ROMP was maintained even for MMs with large MWs. Moreover, very high conversions (>90%) were achieved within 5 min for [M/C] = 50 and within 20 min for [M/C] = 200 at room temperature, further revealing the extraordinary activity of catalyst **3**. Longer reaction times resulted in almost quantitative conversion (>97%) of MMs to brush polymers, while PDIs remained very low (≤1.02).

(A)

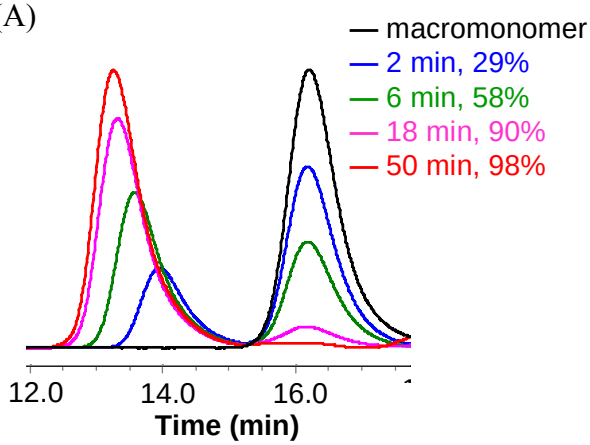

(B)

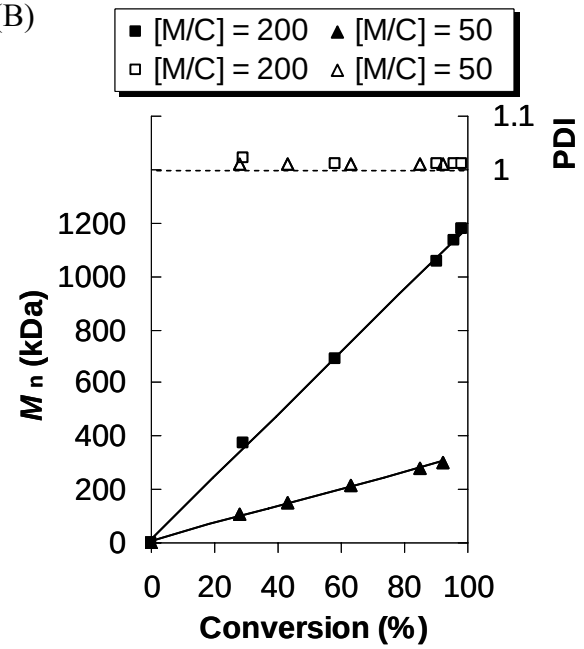

(C)

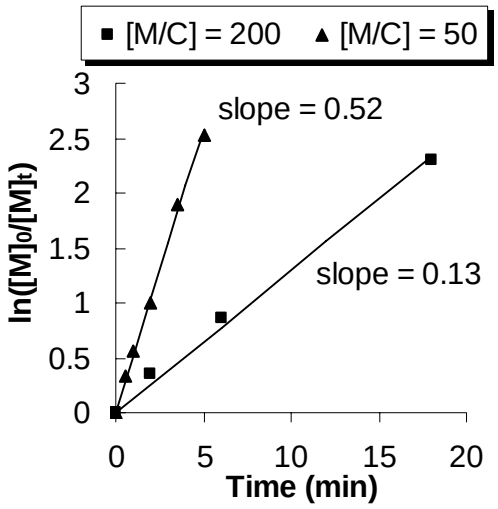

Figure 2. (A) Evolution of GPC traces during ROMP of NB(P*t*BA)4.7k; (B) Dependence of M_n and PDI on MM conversion, and (C) dependence of $\ln([M]_0/[M]_t)$ on time. Conditions: $[M]_0 = 0.05$ M in THF at room temperature.

The MW of the brush polymer, PNB-*g*-P*t*BA, could be controlled by the [M/C] ratio and was slightly higher than the theoretical values, especially when high [M/C] ratios were used. However, the MW was still proportional to the [M/C] ratio (Entry 1-4 in Table 2). GPC traces of the brush polymers obtained at different [M/C] ratios showed a consistent shift toward high MW as increasing the [M/C] ratio, while the peak remained as narrowly dispersed as the macromonomer (Figure 3).

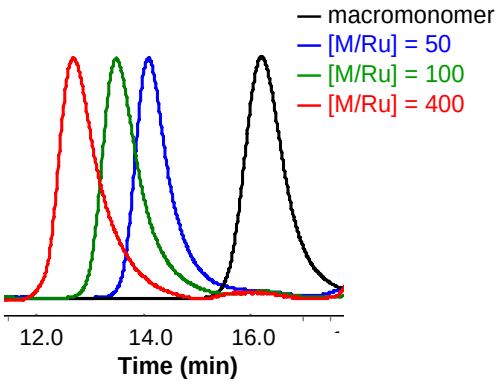

Figure 3. GPC traces of macromonomer NB(P*t*BA)4.7k (black) and crude brush polymers PNB-*g*-P*t*BA obtained at [M/C] = 50 (blue), 100 (green), and 400 (red). Conditions: $[M]_0 = 0.05$ M in THF at room temperature.

All other types of MMs were polymerized similarly using catalyst **3** at varying [M/C] ratios with olefin concentrations of 0.05 – 0.1 M in THF at room temperature (Scheme 4). As shown in Table 2, all of the brush polymers obtained had very narrow PDIs between 1.0 and 1.1 up to MWs of over 2000 kDa, regardless of the MW, functionality, and conversion of the MMs. The very low PDIs of these brush polymers are likely a result of the narrowly dispersed side chains and the highly efficient polymerization of MMs, leading to complete grafting coverage on the polymer backbone. Conversions of MMs to brush polymers were very high (i.e., >90%) in most cases and only weak residual MM peaks were noticeable by GPC. Conversions decreased slightly with increasing [M/C] ratios and increasing MWs of the MMs. However, the small amount of residual MMs can be easily removed simply through precipitation of the polymer solutions into selective solvents due to the large difference in MW between MMs and brush polymers.

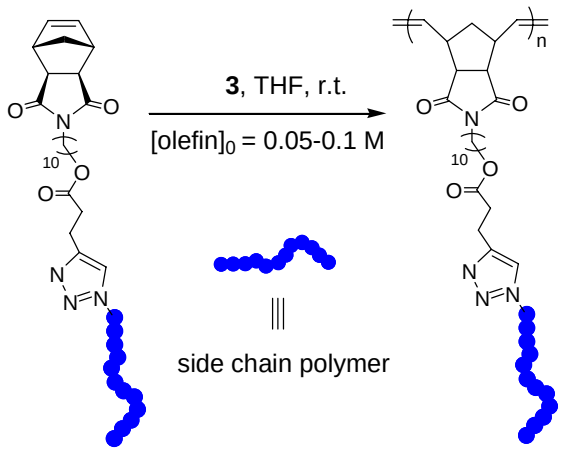

Scheme 4. Synthesis of polymacromonomer from ω-norbornenyl MM.

Table 2. ROMP of macromonomers using catalyst 3

Entry	Macromonomer	[M/C][a]	$M_{n,\ theo}$ (kDa)[b]	$M_{n,\ GPC}$ (kDa)[c]	PDI[c]	DP_{GPC}[d]	Conversion[e]
1	**NB(P*t*BA)4.7k**	50	230	267	1.02	57	98%
2	**NB(P*t*BA)4.7k**	100	461	647	1.01	137	98%
3	**NB(P*t*BA)4.7k**	200	921	1140	1.01	242	98%
4	**NB(P*t*BA)4.7k**	400	1 842	2 620	1.03	557	97%
5	**NB(PMA)3.7k**	50	176	202	1.02	55	95%
6	**NB(PMA)3.7k**	100	348	420	1.02	114	94%
7	**NB(PMA)3.7k**	200	703	891	1.03	241	95%
8	**NB(PMA)3.7k**	400	1 287	1 687	1.05	456	87%
9	**NB(PS)2.2k**	100	210	231	1.02	105	93%
10	**NB(PS)2.2k**	200	427	534	1.03	243	97%
11	**NB(PS)2.2k**	400	836	1271	1.07	578	95%
12	**NB(PS)6.6k**	50	330	348	1.01	53	93%
13	**NB(PS)6.6k**	100	607	701	1.01	106	92%
14	**NB(PS)6.6k**	200	1 162	1 478	1.02	224	88%

[a]MM to catalyst **3** ratio. [b]$M_{n,\ theo} = M_{n,\ GPC}$ (MM) x [M/C] x conversion. [c]Determined by GPC in THF using RI and MALLS detectors. [d]DP of brush polymer = $M_{n,\ GPC}$ (brush polymer)/$M_{n,\ GPC}$ (MM). [e]Conversion of MM to brush polymer is determined by comparing the peak areas of brush polymer and residual MM from GPC measurement of the crude product.

Some of the MMs were polymerized using cyclic catalysts. Due to the relatively low activity, catalysts with unsaturated NHC backbone (**UC-5** and **UC-6**) did not give measurable amount of brush polymer product by GPC. **SC-5** gave conversions of 43%

and 61% for NB(PS)6.6k and NB(PLA)4.7k, respectively, after 6 h at 55 °C in THF (Table 3). Prolonged heating did not further increase the conversions.

Table 3. REMP of macromonomers using SC-5.

Macromonomer	[M/**SC-5**][a]	$M_{n,\,GPC}$ (kDa)[b]	PDI[b]	Conversion[c]
NB(PS)6.6k	50	10 200	1.06[d]	43%
NB(PLA)4.7k	50	7 440	1.42	61%

[a]MM to catalyst **3** ratio, 55 °C in THF. [b]Determined by GPC in THF using RI and MALLS detectors. Only the brush polymer peak was selected to determine the PDI. [c]Conversion of MM to brush polymer is determined by comparing the peak areas of brush polymer and residual MM from GPC measurement of the crude product. [d]The artificially low PDI is because the extremely high MW has exceeded the separable MW range.

AFM of Brush Polymers. We used tapping-mode atomic force microscopy (AFM) to directly visualize individual brush polymers. Visualization of densely grafted brush polymers is facilitated by the large side chains, which prevent coiling of the brush polymer backbone due to the high steric congestion. But individual polymer imaging can be technically challenging: 1) Spin-casting a dilute polymer solution is necessary to disperse individual polymers on the surface for imaging. 2) Favorable polymer-surface interaction is another requirement to have stretched polymers on the surface, otherwise polymers would collapse and coil up to minimize their contact with the surface. 3) Atomically flat surfaces have to be used because as polymer side chains spread on the surface, their thickness is usually only ca. 1 nm. The common commercially available, atomically flat surfaces are highly oriented pyrolytic graphite (HOPG) (for hydrophobic polymers) and mica (for more hydrophilic polymers). The most successful imaging came from the PS grafted polynorbornene (PNB-*g*-PS) with the highest MW (Entry 14 in Table

2) that was spin-cast on HOPG (Figure 4). AFM revealed cylindrical shapes which were expected from the densely grafted nature of the polyMMs. These wormlike polymer brushes also had uniform length and width distributions as a result of their low PDI. Measuring multiple polymer brushes gave an average contour length of 140 nm, a width of 30 nm, and a height of 1 nm. With a backbone DP = 224, the length per monomeric unit, l_m, was calculated to be 0.62 nm. Considering each polynorbornene repeating unit has five backbone carbons, an average two-carbon distance in the polynorbornene brush polymer is 0.25 nm, corresponding to the value for a fully stretched all *trans* -CH_2-CH_2- bond conformation, l_{max}, of 0.25 nm.[5] Therefore, the dimensions of the brush polymers suggest an almost fully extended backbone conformation with side chains stretched and flattened on the surface, presumably as a result of significant steric repulsion of side chains that are grafted on every repeating unit of the backbone.

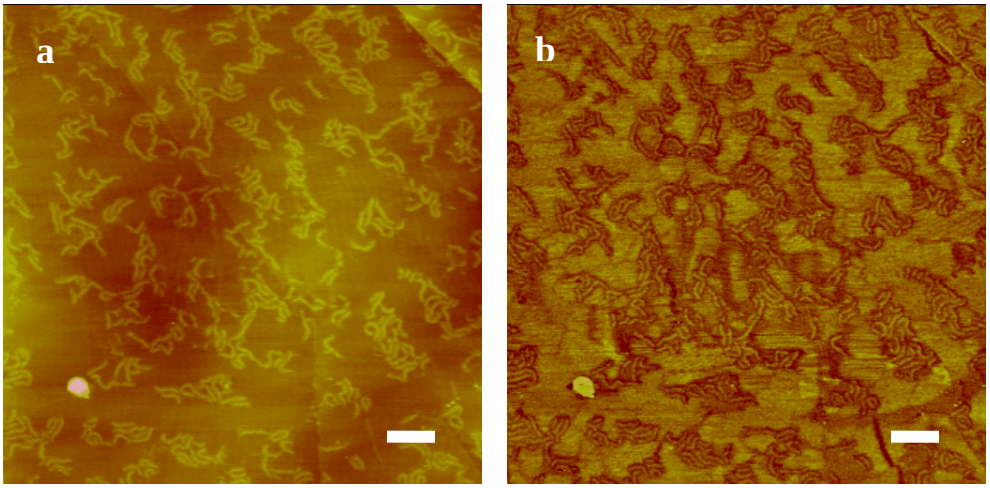

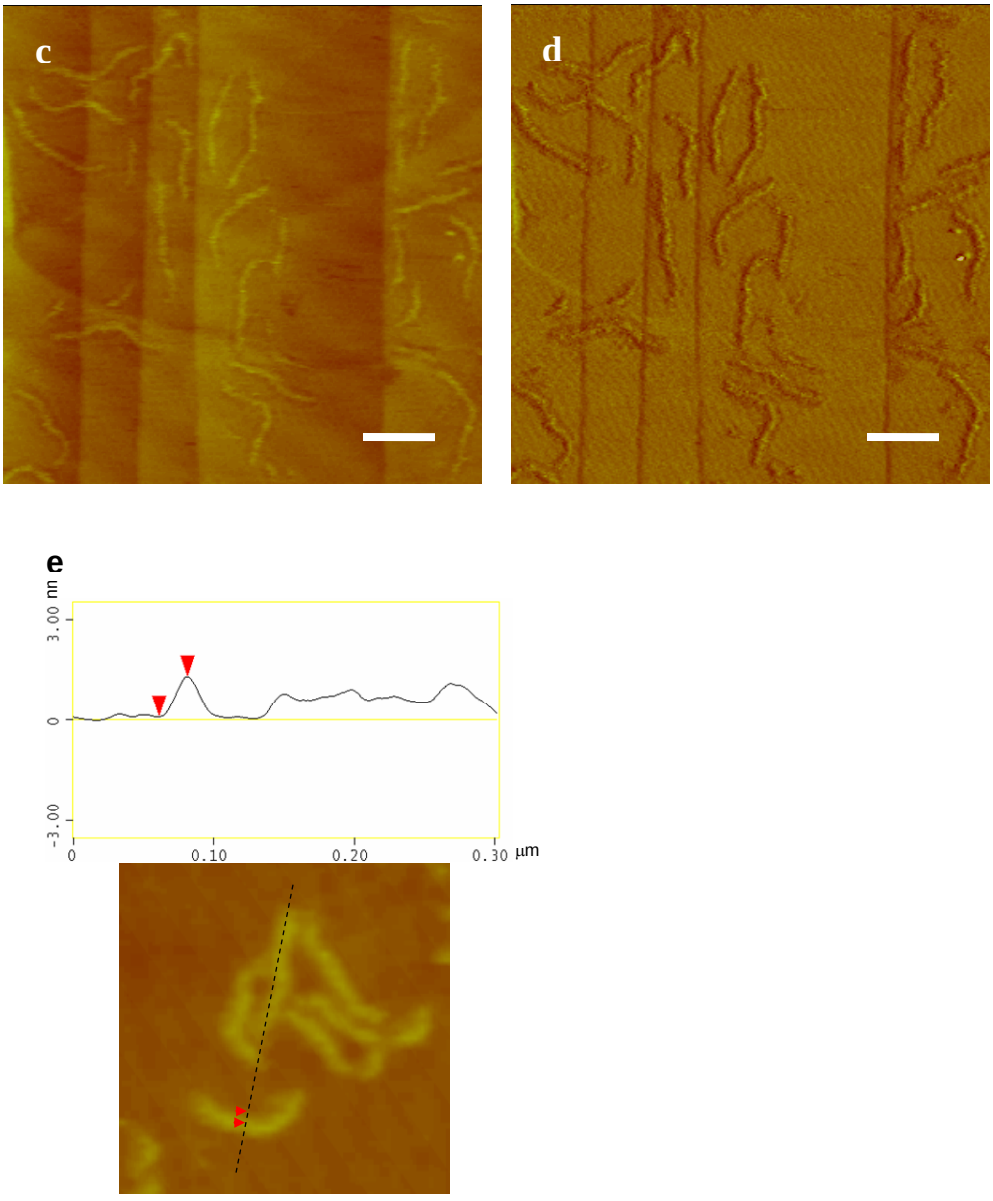

Figure 4. Tapping mode AFM images of brush polymer PNB-*g*-PS (Entry 14 in Table 2) spin-cast from chloroform solution onto HOPG. (a, b) Large scale height and phase images, bar = 300 nm; (c, d) enlarged height and phase images, bar = 100 nm; (e) cross-sectional analysis of an individual polymer brush.

Cyclic PNB-*g*-PS was imaged under the same conditions on HOPG. AFM clearly revealed cyclic structures for some of the brush polymers with open pores as a result of an extended backbone. The cyclic brush polymers had various diameters ranging from 100-300 nm, a reflection of the broad MW distribution of the samples. However, they all

poseesed a uniform width of ~30 nm and a thickness of 1 nm, the same as the linear brush polymers. Unfortunately, linear chain impurities were always observed together with the cyclic structures, and the length of the linear chains varied greatly from 100 nm to >1 μm (Figure 5A). We suspected that a small amount of linear olefin (such as residual monomer from ATRP) in the MM could potentially introduce the linear impurity during ROMP. To test this hypothesis, we synthesized MMs from non-olefinic monomers such as polylactide (PLA) (details on synthesis is in Chapter 5). Brush polymers prepared using NB-PLA and **SC-5** were imaged on freshly cleaved mica by AFM. The imaging quality for these PLA type polymers on mica was generally poor, but both very large cyclic and linear structures (>1 μm in contour length) were again observed (Figure 5B). Therefore, we reasoned that it was not the residual olefin monomer that introduced linear impurity.

There are other possible sources of linear polymer contamination: 1) catalyst decomposition during REMP of MMs; 2) metallocycle opening during REMP due to the highly strained brush polymer backbone; 3) opening of the cyclic polymers by carbon-carbon bond cleavage due to the shear force during spin coating or the surface tension on AFM substrates during imaging. Sheiko, Matyjaszewski, and co-workers reported surface tension-induced degradation of P*n*BA brush polymers, especially for those with long side chains ($DP_{side\ chain}$ = 140).[55,56] This bond cleavage was attributed to the attractive interaction between the spreading side chains and the substrate, which in turn induces tension along the polymer backbone. Any single chain rupture event on cyclic brush polymers will lead to the formation of linear chains. Whether the chain rupture

accounts, to some degree, for the linear contamination and what effect the side chain length has on the cyclic polymer purity warrant detailed investigation in the future.

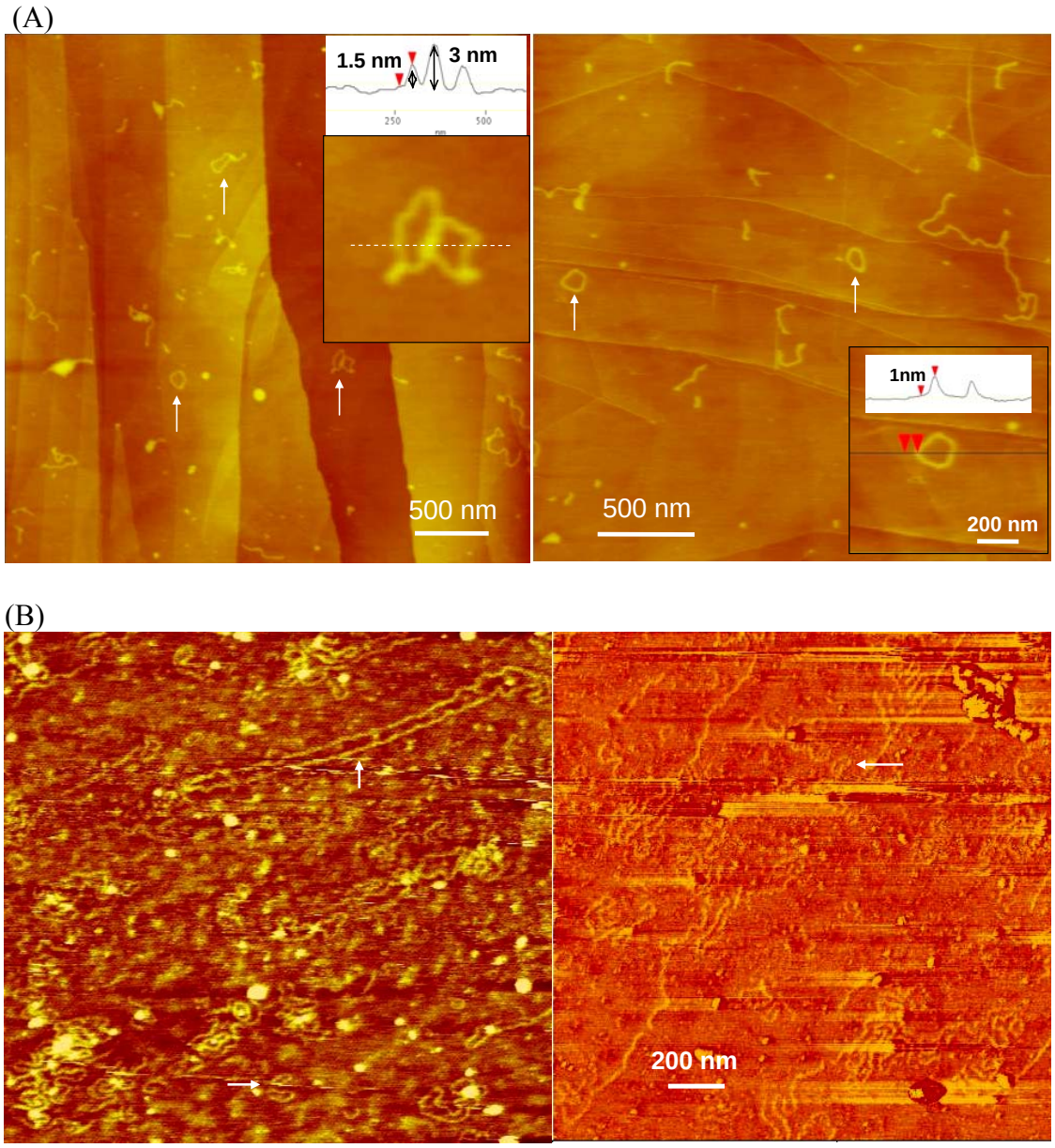

Figure 5. Tapping mode AFM images of cyclic brush polymers (A) PNB-*g*-PS (Entry 1 in Table 3) on HOPG and (B) PNB-*g*-PLA (Entry 2 in Table 3) on mica.

Conclusions

We have efficiently synthesized a series of MMs by "click" coupling of narrowly dispersed azido-terminated pre-polymers with propargyl norbornene. The ROMP of MMs using pyridine-containing ruthenium catalyst **3** has been found to be a general and highly efficient "grafting through" route for the synthesis of a variety of narrowly dispersed brush polymers. The ROMP of MMs exhibited first-order kinetics with respect to the MM concentration up to almost quantitative conversions (>95%) of MMs. MWs of brush polymers increased linearly with MM conversions and were approximately proportional to the ratios of MM to catalyst. Because of the high efficiency, easy experimental procedure, high functional group tolerance of the reported modular approach involving ROMP and "click" chemistry, it allows facile access to a variety of well-defined brush polymers with a broad range of functionalities and MWs.

Experimental Section

Materials. THF was purified by passing through solvent purification columns. $(H_2IMes)(pyr)_2(Cl)_2RuCHPh$ (**3**) was prepared according to a literature procedure.[54] *cis*-5-norbornene-*exo*-2,3-dicarboxylic anhydride was prepared as described previously.[37] St, MA, and *t*-BA were passed through a column of basic alumina immediately before use. All other materials were obtained from commercial sources and used as received. Azido-terminated pre-polymers, PMA (M_n = 3 270 g/mol and PDI = 1.03), P*t*BA (M_n = 4 100 g/mol and PDI = 1.03), and PS (M_n = 1 800 g/mol and PDI = 1.03; M_n = 6 200 g/mol and PDI = 1.03) were synthesized according to literature procedures.[16,49]

Characterizations. ^{1}H and ^{13}C NMR spectra were recorded in $CDCl_3$ using a Varian Mercury 300 or Varian Inova 500 spectrometer. Chemical shifts are reported in ppm relative to $CDCl_3$ ($\delta = 7.27$).

High-resolution mass spectra (FAB) were provided by California Institute of Technology Mass Spectrometry Facility.

Gel permeation chromatography (GPC) was carried out in THF on two PLgel 10 μm mixed-B LS columns (Polymer Laboratories) connected in series with a DAWN EOS multiangle laser light scattering (MALLS) detector and an Optilab DSP differential refractometer (both from Wyatt Technology). No calibration standards were used, and d*n*/d*c* values were obtained for each injection by assuming 100% mass elution from the columns.

Atomic Force Microscopy (AFM) images were taken using a Nanoscope IV Scanning Probe Microscope Controller (Digital Instruments, Veeco Metrology Group) in tapping mode in air at room temperature using silicon tips (spring constant = 40-50 N/m, resonance frequency = 170-190 kHz, and tip radius of curvature <10 nm). The samples were prepared by spin casting dilute solutions (0.01 wt%) in chloroform onto freshly cleaved highly oriented pyrolytic graphite.

***N*-(hydroxydecanyl)-*cis*-5-norbornene-*exo*-2,3-dicarboximide.**

A round-bottom flask was charged with *cis*-5-norbornene-exo-2,3-dicarboxylic anhydride (0.95 g, 5.8 mmol) and 10-amino-1-decanol (1.0 g, 5.8 mmol). To the flask was added 20 mL toluene, followed by triethylamine (80 μL, 0.58 mmol). A homogeneous solution was obtained upon heating. A Dean-Stark trap was attached to the flask, and the reaction mixture was heated at reflux (135 ºC) for 4 h. The reaction mixture was then cooled and

concentrated *in vacuo* to yield an off-white solid. This residue was dissolved in 20 mL CH_2Cl_2 and washed with 0.1 N HCl (10 mL) and brine (10 mL). The organic layer was dried over $MgSO_4$ and concentrated *in vacuo* to yield 1.8 g colorless, viscous oil (97% yield). ^{1}H NMR (500 MHz, $CDCl_3$): δ 1.20-1.28 (m, 13H), 1.49-1.56 (m, 5H), 2.65 (d, J = 1.5 Hz, 2H), 3.26 (t, J = 1.5 Hz, 2H), 3.44 (t, J = 7.5 Hz, 2H), 3.62 (t, J = 6.5 Hz, 2H), 6.27 (t, J = 2.0 Hz, 2H). ^{13}C NMR (125 MHz, $CDCl_3$): δ 25.9, 27.1, 27.9, 29.3, 29.5, 29.5, 29.6, 33.0, 39.0, 42.9, 45.4, 48.0, 63.3, 138.1, 178.4. HRMS (FAB+) *m/z* calcd for $C_{19}H_{30}O_3N$ $[M+H]^+$: 320.2226, found 320.2238.

***N*-(pentynoyl decanyl)-*cis*-5-norbornene-*exo*-2,3-dicarboximide 4.**

To a round-bottom flask was added N-(hydroxydecanyl)-*cis*-5-norbornene-exo-2,3-dicarboximide (0.80 g, 2.5 mmol), N-(3-dimethylaminopropyl)-N'-ethylcarbodiimide hydrochloride (EDC) (0.58 g, 3.0 mmol) and 4-dimethylaminopyridine (DMAP) (0.10 g, 0.82 mmol), followed by 10 mL CH_2Cl_2. Pentynoic acid (0.25 g, 2.5 mmol) was added as a solution in 5 mL CH_2Cl_2 via syringe. The reaction mixture was allowed to stir under argon at room temperature overnight. The reaction mixture was washed with water (2x20 mL) and brine (20 mL) and dried over $MgSO_4$. The solvent was evaporated and the remaining residual was purified by silica gel chromatography (ethyl acetate/hexanes, 3:7 v/v) to give 0.81 g **4** as a colorless oil (81% yield). ^{1}H NMR (500 MHz, $CDCl_3$): δ 1.22-1.33 (m, 13H), 1.50-1.55 (m, 3H), 1.62 (t, J = 7.5 Hz, 2H), 1.98 (t, J = 2.5 Hz, 1H), 2.17-2.56 (m, 4H), 2.67 (d, J = 1.5 Hz, 2H), 3.27 (t, J = 1.5 Hz, 2H), 3.45 (t, J = 7.5 Hz, 2H), 4.09 (t, J = 7 Hz, 2H), 6.28 (t, J = 2.0 Hz, 2H)1H). ^{13}C NMR (125 MHz, $CDCl_3$): δ 14.6, 26.1, 27.2, 28.0, 28.8, 29.3, 29.4, 29.5, 29.6, 33.6, 39.0, 42.9, 45.4, 48.0, 65.1, 69.2, 82.8,

138.1, 172.1, 178.4. HRMS (FAB+) *m/z* calcd for $C_{24}H_{34}O_4N$ $[M+H]^+$: 400.2488, found 400.2505.

General procedure for synthesis of macromonomers via "click" coupling of pre-polymer and 4. In a typical experiment, to a 20 mL scintillation vial was added 1 g azido-terminated pre-polymer, the desired amount of **4** (1 eq. to pre-polymer end group) and CuBr (0.1 eq to **4**), and a stir bar. The vial was then degassed and 10 mL degassed anhydrous THF was added via syringe under an argon atmosphere. PMDETA (1 eq to CuBr) was injected via a microsyringe. The reaction vial was stirred at 50 ºC under argon overnight. The reaction mixture was then passed through a short neutral alumina column to remove the catalyst. The resulting macromonomers were isolated by precipitation into MeOH for NB-PS or by removal of the solvent under high vacuum for NB-P*t*BA.

General procedure for ROMP of macromonomers. In a typical experiment, an oven-dried small vial was charged with 100 mg macromonomer and a stir bar. The vial was then degassed, and the desired amount of degassed, anhydrous THF ($[M]_0$ = 0.05-0.10 M) was added via syringe under an argon atmosphere to dissolve the macromonomer. A stock solution of catalyst **3** in degassed, anhydrous THF was prepared in a separate vial. The desired amount of catalyst was injected into the macromonomer solution to initiate the polymerization. The reaction vial was stirred at room temperature under argon. After the polymerization was complete, the reaction mixture was quenched with one drop of ethyl vinyl ether. A small sample was withdrawn for GPC measurement. The rest of the reaction mixture was then diluted and precipitated into 10 mL stirring MeOH for PNB-*g*-(PS) and PNB-*g*-(PMA) and MeOH/water (4:1) for PNB-*g*-(P*t*BA). Trace amount of residual macromonomer can be readily removed via precipitation into MeOH,

MeOH/water (4:1), and cyclohexane/heptane (1:2) for PNB-*g*-(PMA), PNB-*g*-(P*t*BA), and PNB-*g*-(PS) respectively. The resulting brush polymers were dried *in vacuo*.

References

(1) Percec, V.; Ahn, C. H.; Ungar, G.; Yeardley, D. J. P.; Moller, M.; Sheiko, S. S. *Nature* **1998**, *391*, 161-164.

(2) Hadjichristidis, N. P., M.; Pispas, S.; Iatrou, H. *Chem. Rev.* **2001**, *101*, 3747.

(3) Zhang, M.; Müller, A. H. E. *J. Polym. Sci., Part A: Polym. Chem.* **2005**, *43*, 3461-3481.

(4) Wintermantel, M.; Gerle, M.; Fischer, K.; Schmidt, M.; Wataoka, I.; Urakawa, H.; Kajiwara, K.; Tsukahara, Y. *Macromolecules* **1996**, *29*, 978-983.

(5) Sheiko, S. S.; Möller, M. *Chem. Rev.* **2001**, *101*, 4099-4124.

(6) Beers, K. L.; Gaynor, S. G.; Matyjaszewski, K.; Sheiko, S. S.; Möller, M. *Macromolecules* **1998**, *31*, 9413-9415.

(7) Börner, H. G.; Beers, K.; Matyjaszewski, K.; Sheiko, S. S.; Möller, M. *Macromolecules* **2001**, *34*, 4375-4383.

(8) Cheng, G.; Böker, A.; Zhang, M.; Krausch, G.; Müller, A. H. E. *Macromolecules* **2001**, *34*, 6883.

(9) Zhang, M.; Breiner, T.; Mori, H.; Müller, A. H. E. *Polymer* **2003**, *44*, 1449-1458.

(10) Kriegel, R. M.; Rees, W. S.; Weck, M. *Macromolecules* **2004**, *37*, 6644-6649.

(11) Runge, M. B.; Dutta, S.; Bowden, N. B. *Macromolecules* **2006**, *39*, 498-508.

(12) Neugebauer, D.; Sumerlin, B. S.; Matyjaszewski, K.; Goodhart, B.; Sheiko, S. S. *Polymer* **2004**, *45*, 8173-8179.

(13) Sumerlin, B. S.; Neugebauer, D.; Matyjaszewski, K. *Macromolecules* **2005**, *38*, 702-708.

(14) Deffieux, A.; Schappacher, M. *Macromolecules* **1999**, *32*, 1797-1802.

(15) Schappacher, M.; Deffieux, A. *Macromolecules* **2005**, *38*, 7209-7213.

(16) Gao, H.; Matyjaszewski, K. *J. Am. Chem. Soc.* **2007**, *129*, 6633-6639.

(17) Schappacher, M.; Deffieux, A. *Science* **2008**, *319*, 1512-1515.

(18) Tsukahara, Y. M., K.;Segawa, A.;Yamashita, Y. *Macromolecules* **1989**, *22*, 1546-1552.

(19) Tsukahara, Y. T., K.;Yamashita, Y.;Shimada, S. *Macromolecules* **1990**, *23*, 5201-5208.

(20) Dziezok, P.; Sheiko, S. S.; Fischer, K.; Schmidt, M.; Möller, M. *Angew. Chem. Int. Ed.* **1997**, *36*, 2812-2815.

(21) Neiser, M. W.; Okuda, J.; Schmidt, M. *Macromolecules* **2003**, *36*, 5437-5439.

(22) Neiser, M. W.; Muth, S.; Kolb, U.; Harris, J. R.; Okuda, J.; Schmidt, M. *Angew. Chem. Int. Ed.* **2004**, *43*, 3192-3195.

(23) Yamada, K.; Miyazaki, M.; Ohno, K.; Fukuda, T.; Minoda, M. *Macromolecules* **1999**, *32*, 290-293.

(24) Pantazis, D.; Chalari, I.; Hadjichristidis, N. *Macromolecules* **2003**, *36*, 3783-3785.

(25) Heroguez, V.; Breunig, S.; Gnanou, Y.; Fontanille, M. *Macromolecules* **1996**, *29*, 4459-4464.

(26) Heroguez, V.; Gnanou, Y.; Fontanille, M. *Macromolecules* **1997**, *30*, 4791-4798.

(27) Heroguez, V.; Amedro, E.; Grande, D.; Fontanille, M.; Gnanou, Y. *Macromolecules* **2000**, *33*, 7241-7248.

(28) Nomura, K.; Takahashi, S.; Imanishi, Y. *Polymer* **2000**, *41*, 4345-4350.

(29) Nomura, K.; Takahashi, S.; Imanishi, Y. *Macromolecules* **2001**, *34*, 4712-4723.

(30) Murphy, J. J.; Nomura, K. *Chem. Commun.* **2005**, 4080-4082.

(31) Liaw, D.-J.; Huang, C.-C.; Ju, J.-Y. *J. Polym. Sci., Part A: Polym. Chem.* **2006**, *44*, 3382-3392.

(32) Hilf, S.; Kilbinger, A. F. M. *Macromol. Rapid Comm.* **2007**, *28*, 1225-1230.

(33) Jha, S.; Dutta, S.; Bowden, N. B. *Macromolecules* **2004**, *37*, 4365-4374.

(34) Bielawski, C. W.; Grubbs, R. H. *Angew. Chem. Int. Ed.* **2000**, *39*, 2903-2906.

(35) Choi, T.-L.; Grubbs, R. H. *Angew. Chem. Int. Ed.* **2003**, *42*, 1743-1746.

(36) Camm, K. D.; Castro, N. M.; Liu, Y.; Czechura, P.; Snelgrove, J. L.; Fogg, D. E. *J. Am. Chem. Soc.* **2007**, *129*, 4168-4169.

(37) Matson, J. B.; Grubbs, R. H. *J. Am. Chem. Soc.* **2008**, *130*, 6731-6733.

(38) Rajaram, S.; Choi, T.-L.; Rolandi, M.; Fréchet, J. M. J. *J. Am. Chem. Soc.* **2007**, *129*, 9619-9621.

(39) Hawker, C. J.; Bosman, A. W.; Harth, E. *Chem. Rev.* **2001**, *101*, 3661-3688.

(40) Matyjaszewski, K.; Xia, J. *Chem. Rev.* **2001**, *101*, 2921-2990.

(41) Kamigaito, M.; Ando, T.; Sawamoto, M. *Chem. Rev.* **2001**, *101*, 3689-3746.

(42) Cheng, C.; Khoshdel, E.; Wooley, K. L. *Macromolecules* **2005**, *38*, 9455-9465.

(43) Patton, D. L.; Advincula, R. C. *Macromolecules* **2006**, *39*, 8674-8683.

(44) Gao, H.; Louche, G.; Sumerlin, B. S.; Jahed, N.; Golas, P.; Matyjaszewski, K. *Macromolecules* **2005**, *38*, 8979-8982.

(45) Lutz, J.-F.; Börner, H. G.; Weichenhan, K. *Macromol. Rapid Comm.* **2005**, *26*, 514-518.

(46) Golas, P. L.; Tsarevsky, N. V.; Sumerlin, B. S.; Matyjaszewski, K. *Macromolecules* **2006**, *39*, 6451-6457.

(47) Lutz, J.-F.; Börner, H. G.; Weichenhan, K. *Macromolecules* **2006**, *39*, 6376-6383.

(48) Whittaker, M. R.; Urbani, C. N.; Monteiro, M. J. *J. Am. Chem. Soc.* **2006**, *128*, 11360-11361.

(49) Vogt, A. P.; Sumerlin, B. S. *Macromolecules* **2006**, *39*, 5286-5292.

(50) Binder, W. H.; Kluger, C. *Macromolecules* **2004**, *37*, 9321-9330.

(51) Asrar, J. *Macromolecules* **1992**, *25*, 5150-5156.

(52) Rule, J. D.; Moore, J. S. *Macromolecules* **2002**, *35*, 7878-7882.

(53) Pollino, J. M.; Stubbs, L. P.; Weck, M. *Macromolecules* **2003**, *36*, 2230-2234.

(54) Love, J. A.; Morgan, J. P.; Trnka, T. M.; Grubbs, R. H. *Angew. Chem., Int. Ed.* **2002**, *41*, 4035–4037.

(55) Sheiko, S. S.; Sun, F. C.; Randall, A.; Shirvanyants, D.; Rubinstein, M.; Lee, H.; Matyjaszewski, K. *Nature* **2006**, *40*, 191–194.

(56) Lebedeva, N. V.; Sun, F. C.; Lee, H.; Matyjaszewski, K.; Sheiko, S. S. *J. Am. Chem. Soc.* **2008**, *130*, 4228–4229.